Oxidative Damage Generated by an Oxo-Metalloporphyrin onto the Human Telomeric Sequence†

Corine Vialas, Geneviève Pratviel, and Bernard Meunier*

Laboratoire de Chimie de Coordination du CNRS, 205 route de Narbonne, 31077 Toulouse Cedex 4, France

Received April 3, 2000; Revised Manuscript Received June 1, 2000

ABSTRACT: The cationic metalloporphyrin Mn-TMPyP activated by $KHSO_5$ has been used as cleaver of an oligonucleotide containing the four human telomere repeats of 5′-GGGTTA. This oligonucleotide formed an intramolecular quadruplex DNA under 200 mM KCl as probed by DMS footprinting and could fold into different quadruplex structures under 200 mM NaCl. We found that the oxo-metalloporphyrin was able to mediate efficient oxidative cleavage of the quadruplex. The location of damage showed that the metalloporphyrin was able to bind to the last G-tetrad of the quadruplex structure via an external interaction. This metalloporphyrin-G-tetrad interaction needs a relatively high flexibility of the single-stranded linker regions to allow the partial stacking of the metalloporphyrin with the last G-tetrad planar structure. The oxidative damage consisted of guanine oxidation within the interacting G-tetrad together with an 1′-carbon hydroxylation of deoxyribose residues of the thymidine residues located on the neighboring single-stranded loop. So the high-valent oxo-metalloporphyrin is able to mediate both electron-abstraction or H-abstraction on G or T residues, respectively, within the DNA quadruplex target.

Telomeres are short nucleotidic repeats located at the end of chromosomes, essential to maintain genetic integrity (*1*, *2*). They are specialized nucleoprotein complexes that have important functions in the protection of chromosome ends from degradation or end-to-end fusion. They also allow chromosomic DNA to be completely replicated without loss of genetic material. The telomeric DNA sequences known from a large number of organisms generally consist of many tandem repeats of G-rich sequences. The sequence of a repeating unit of human telomeres is 5′-GGGTTA (*3*). Although the bulk of telomeric DNA is double-stranded, the extreme terminus contains a 3′ single-stranded overhang (*4*). In G-rich single-stranded DNA, the guanines form Hoogsteen base pairs which can associate to induce cyclic tetrads formation called G-tetrads. Each G-tetrad consists of four guanine bases in a square planar array arranged in a cyclic hydrogen-bonding pattern, where each guanine is both the donor and acceptor of two hydrogen bonds (Figure 1A). This characteristic folding can lead to quadruplex DNA formation (Figure 1B) (*1*). Although G-rich strands associate to form cyclic tetrads in physiological conditions, their formation and stability is increased by the presence of monovalent cations such as K^+ and Na^+ (*5*−*8*). Indeed, the unique feature of the G-tetrad as a structural motif is a pocket with its center containing electron-rich carbonyl oxygens able to interact with these cations. K^+ ions are better to stabilize G-tetrads than Na^+ ions (*9*−*12*). The higher affinity of potassium salt for the telomeric sequence can be explained by a better fit of its ionic radius for the quadruplex structure compared to sodium salt.

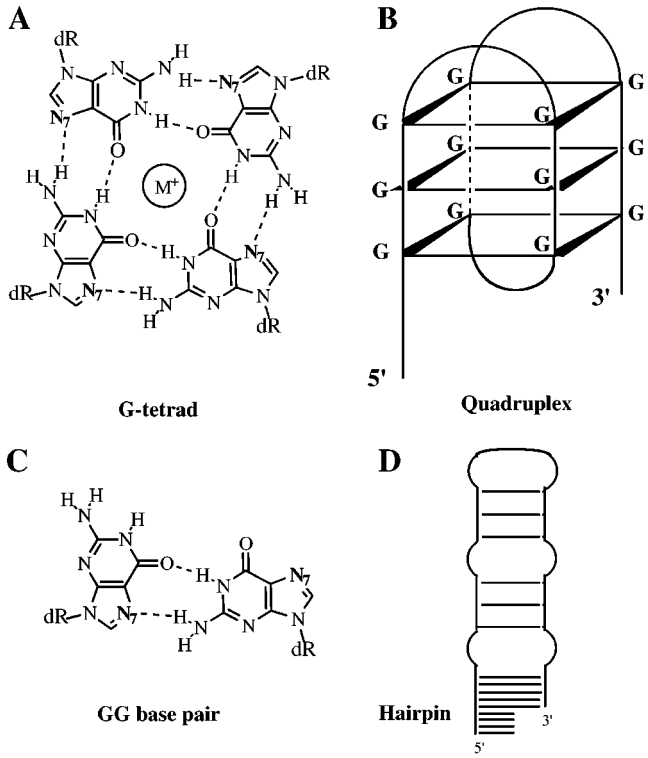

FIGURE 1: (A) Structure of an individual G-tetrad showing the Hoogsteen base pairing. M^+ represents a monovalent cation such K^+ or Na^+ and dR the sugar−phosphate backbone. (B) Schematic representation showing the possible folded intramolecular quadruplex structure. (C) GG-base pair formed by the means of Hoogsteen hydrogen bonds. (D) Intramolecular hairpin.

Evidence indicates that telomeric DNA shortens during the growth of various human somatic cells. These loss of telomeric repeat after each cell division may be a biological clock limiting the proliferative lifespan of somatic cells (*13*,

† Corine Vialas is indebted to the "Ligue Nationale Contre le Cancer, Section du Gers" for a PhD fellowship.

* To whom correspondence should be addressed. Phone: +33(0)561333146. Fax: +33(0)561553003. E-mail: bmeunier@lcc-toulouse.fr.

10.1021/bi000743x CCC: $19.00
Published on Web 07/13/2000

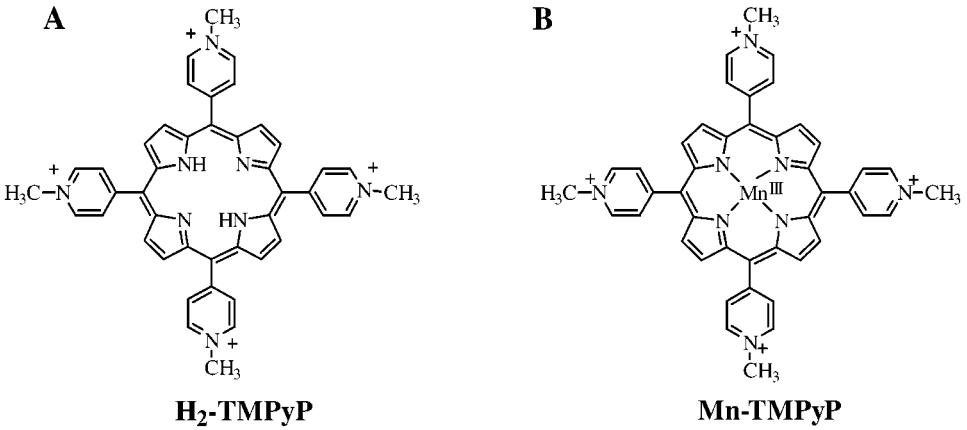

FIGURE 2: Structures of two cationic porphyrin derivatives: (A) the nonmetalated H_2-TMPyP and (B) the metalated Mn-TMPyP. This latter complex exhibits two water molecules as axial ligands and is surrounded by five acetate counterions.

14). From the moment that telomere length would become smaller than a critical size, cells would stop dividing, become senescent, and die. On the other hand, the majority of the immortal cells do not present telomeric shortening during cellular divisions (*15*). To compensate for the sequence loss that results from incomplete terminal replication, immortalized cells, tumor cells and germline cells express an enzyme, the telomerase, which synthesizes the missing telomeric sequences (*16*). Consequently, telomerase of cancer cells is an attractive target for the development of new drugs able to reduce telomere length by inhibition of the enzyme activity (*2*). Several agents interacting with the characteristic G-rich secondary structures -(GGGTTA)- of telomeric DNA have been developed (*17*−*20*). Such compounds studied in Hurley's group have shown high affinity for those structures, forming stable complexes by stacking with the tetrad that may inhibit the recognition of telomeric DNA by telomerase.

The tetracationic porphyrin, *meso*-tetrakis(4-*N*-methylpyridiniumyl)-porphyrin, H_2-TMPyP[1] (Figure 2A) possesses the appropriate physicochemical properties to interact with the G-quadruplets (*21*−*26*). Indeed, its molecular size is similar to the G-tetrad one. Moreover, this planar compound, that can hydrophobically interact with the tetrad via π-stacking, presents substituents with positive charges favorable for electrostatic interactions with the phosphate backbone. H_2-TMPyP was recently shown to be a potent inhibitor of human telomerase in vitro (*22*). CD and UV thermal melting studies together with photocleavage experiments showed that this porphyrin binds to and stabilizes the human telomeric DNA quadruplex $(GGGTTA)_4$ by external π-stacking with the last guanine tetrad. No intercalation between the tetrads has been highlighted, thus leaving the quadruplex DNA edifice intact (*25*).

The manganese derivative of TMPyP is a powerful artificial nuclease (*27*−*30*). Mn-TMPyP (Figure 2B) can be activated by an oxygen atom donor, potassium monopersulfate $KHSO_5$, into a very reactive high-valent porphyrin Mn(V)═O species (*31*−*33*). This powerful catalytic system is able to oxidize deoxyriboses (*27*, *28*) or guanine residues (*30*) within double-stranded DNA.

[1] Abbreviations: TMPyP, *meso*-tetrakis(4-*N*-methylpyridiniumyl)-porphyrinato dianion; Mn-TMPyP, manganese(III)-bis-aqua-*meso*-tetrakis(4-*N*-methylpyridiniumyl)-porphyrin; 5-MF, 5-methylene-2-furanone; DMS, dimethyl sulfate.

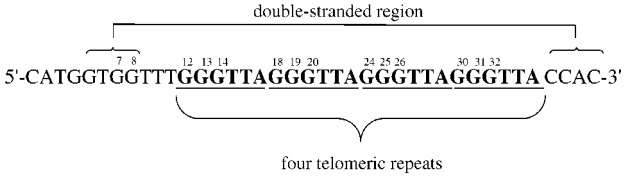

FIGURE 3: human telomeric sequence.

Here, we report the efficient oxidative degradation mediated to the human telomeric sequence by the Mn-TMPyP/$KHSO_5$ system. The oxidative lesions were found to depend on the secondary structure of the telomeric sequence, suggesting that this oxo-manganese porphyrin is a good probe for quadruplex structures of DNA.

EXPERIMENTAL PROCEDURES.

Synthesis, Purification, and Labeling of the Human Telomeric Target. The human telomeric sequence (Figure 3) was synthesized by standard solid-phase β-cyanoethyl phosphoramidite chemistry. Purification was performed by electrophoresis on a 20% polyacrylamide denaturing gel. DNA concentration was determined by UV measurements at 260 nm. The 5′-end of the telomeric target was labeled by ^{32}P using standard procedures with T4 polynucleotide kinase and [γ-^{32}P]ATP purchased from New England Biolabs and ICN Biomedical, respectively.

Dimethyl Sulfate Footprinting. A typical experiment consisted of incubation of the 5′-^{32}P-labeled human telomeric sequence (1 μM, 100000−150000 cpm) in Tris/HCl buffer pH 7 (50 mM), in the presence of KCl (200 mM) (Tris/KCl buffer) or NaCl (200 mM) (Tris/NaCl buffer). Control reactions were done in Tris/HCl buffer pH 7 (50 mM) (Tris buffer). The DNA solution was heated for 10 min at 90 °C and slowly cooled to room temperature. The reaction was initiated by addition of dimethyl sulfate (DMS) (1% final, from Sigma). Total volume was 20 μL. After 2, 5, or 10 min at 0 °C, the reaction was stopped with 80 μL of DMS stop buffer consisting of 2 μL of β-mercaptoethanol from Sigma, 10 μL of 1 mg/mL calf thymus DNA from Sigma, and 68 μL of distilled water. Samples were then diluted with 10 μL of 3.5 M sodium acetate buffer (pH 5.2) and 1 μL of yeast tRNA at 10 mg/mL and precipitated with 300 μL of cold ethanol overnight at −20 °C. After centrifugation (15 min at 4 °C, 12 × 10^3 rpm), the DNA pellet was washed twice with cold ethanol, dried under vacuum (Speedvac),

and subjected to piperidine treatment (50 μL, 1 M, 30 min at 90 °C). Piperidine treatment was followed by lyophilization of the piperidine solution.

Oxidation of the Human Telomeric Sequence by Mn-TMPyP/KHSO$_5$. Telomeric sequence cleavage reactions were performed with 5′-labeled target (final concentration 1 μM, 100000−150000 cpm) in Tris/HCl buffer pH 7 (50 mM), and KCl (200 mM) (Tris/KCl buffer) or NaCl (200 mM) (Tris/NaCl buffer). Experiments were also carried out in 50 mM Tris/HCl buffer pH 7 (Tris buffer). The media were boiled at 90 °C for 10 min and slowly cooled to room temperature. The DNA was preincubated with Mn-TMPyP (1 μM, see ref *34* for preparation) during 15 min at 0 °C. DNA cleavage reactions were initiated by adding a freshly prepared solution of $KHSO_5$ (final concentration 100 μM, Curox from Interox). Final volume was 20 μL. After 1 h (or 5 min) at 0 °C, the reactions were stopped by addition of Hepes buffer pH 8 (48 mM, final concentration). The DNA samples were then subjected to ethanol precipitation and centrifugation as described above. Piperidine treatments performed in some cases on DNA cleavage products were as described above.

After the addition of Hepes buffer, some samples were subjected to further treatment: (i) heating step consisted of a 90 °C heating during 30 min (pH 7.5) before ethanol precipitation. (ii) $NaBH_4$ treatment was performed by incubation of the reaction medium for 30 min at room temperature with $NaBH_4$ (final concentration 0.1 M, Janssen Chimica) and was stopped by further addition of 10 equivalents of acetone (with respect to $NaBH_4$). the samples were ethanol precipitated and a part of them were subjected to a piperidine treatment.

HPLC Analysis of the Oxidative Degradation of Deoxyribose Unit. After typical quadruplex oxidation in Tris/KCl or Tris/NaCl buffer (60-scale fold), the reaction media were analyzed by HPLC. The samples were either directly injected or heated for 15 min at 90 °C, chilled in liquid nitrogen to stop the heated reaction before analysis. The liquid chromatography analysis was performed isocratically on a C18 Uptisphere reverse phase column (from Interchim, France), with methanol/5 mM ammonium acetate buffer pH 4.5, 7/93 at 1 mL/min. Detection was at 260 nm. The retention times for thymine and 5-MF were 12 and 19 min, respectively.

Oxidative cleavage of double-stranded 35-mer. Double-stranded DNA cleavage reactions were performed on a 35-mer duplex which was 5′-^{32}P-end labeled on one or the other strand. Typical experiment was done at a duplex final concentration of 1 μM in Tris buffer pH 8 (40 mM) and NaCl (100 mM). Annealing of the two 35-mer single-strands was achieved by heating at 90 °C for 1 min followed by slow cooling to room temperature. The mixture was then incubated with Mn-TMPyP (final concentration of 1 μM). Cleavage reactions were initiated by the addition of $KHSO_5$ at a final concentration of 100 μM. Total volume was 15 μL. After 1 h at 0 °C, the oxidation reactions were stopped by the addition of Hepes buffer followed by ethanol precipitation as described above.

Polyacrylamide Gel Electrophoresis Analysis. After ethanol precipitation of the reaction samples or after piperidine treatment, the dry DNA pellet was diluted in formamide with marker dyes. The samples were incubated 2 min at 90 °C, chilled in ice, and run on a 20% denaturing polyacrylamide gel (7 M urea) for 3 h at about 2000 V. The DNA fragments were visualized either by autoradiography using Kodak BioMax MR-1 film or by phosphorimagery (Molecular Dynamics) using Image Quant software. Each gel included a Maxam−Gilbert sequencing (G-lane).

Melting Temperature Measurements. Samples were prepared by heating the telomeric sequence alone (1 μM) in Tris/HCl buffer pH 7 (50 mM) and KCl (200 mM) or NaCl (200 mM) at 90 °C for 10 min and gradually cooling to room temperature. The DNA was then preincubated or not with Mn-TMPyP (1 μM) during 15 min. Concentrations in brackets are final concentration. Absorbance versus temperature data were obtained at 260 nm. The temperature was increased with an HP 89090A Peltier temperature controller from 10 to 95 °C. The heating rate was 0.5 °C/min. The melting temperatures were deduced from the corresponding melting curves.

RESULTS AND DISCUSSION

Secondary Structures of the Human Telomeric Sequence Depends on the Cation Present in the Medium. The studied telomeric DNA target (Figure 3) is composed by four human telomeric repeats (5′-GGGTTA) able to fold into an intramolecular quadruplex which can be stabilized by a double-stranded stem as shown previously (25). We performed a dimethyl sulfate (DMS) footprinting analysis in order to check that the telomeric sequence could adopt G-quadruplex structures under the used reaction conditions (buffer, ionic strength). The signature of a G-quartet formation is the strong protection against methylation of the guanine N_7 due to Hoogsteen base pairs (Figure 1A). We studied guanine methylation of the human telomeric target under three different conditions (i) in the presence of K^+ ions (Tris/KCl), (ii) in the presence of Na^+ ions (Tris/NaCl), or (iii) in the absence of those two alkaline monovalent cations (Tris) (data not shown). This experiment allowed us to confirm that the telomeric sequence could fold into different secondary structures depending on the added cation, as already described in the literature (*5*, *6*, *9*, *11*). In the presence of K^+ ions, the observed full protection against methylation of all the guanines of the telomeric sequence, compared to the sensitivity of G_7 and G_8, located in the double-stranded stem, suggested that the target folding is an intramolecular quadruplex (Figure 1B). In the quadruplex structure all the N_7 of guanines are engaged in Hoogsteen hydrogen bonds and thus are not prone to methylation (Figure 1A). On the other hand, the DMS semi-protection patterns observed in the presence of Na^+ ions revealed that the secondary structures formed under these conditions were less tightly bound. This result may be explained by the existence of intramolecular hairpins due to guanine pairings (Figure 1D), where only one N_7 of G is exposed to the solvent (Figure 1C). It is known that different foldings may coexist in Tris/NaCl (*5*, *6*, *9*−*11*, *25*, *35*), intramolecular quadruplex may be associated with intramolecular hairpins. A partial association of these hairpins to form interstrand tetrads three- or six-layered quadruplexes are also possible. In the absence of K^+ and Na^+ cations, the observed full sensitivity of all guanines toward methylation indicated that the human telomeric DNA structure, under these conditions, may be a simple stem-loop where the guanines located either in a single-stranded loop or in a Watson−Crick double-stranded helix could be methylated. In that case all N_7 of the guanines would be

equally prone to methylation. In summary, the different DMS reaction results confirmed that the human telomeric sequence studied here could fold into different secondary structures depending on the reaction medium. An intramolecular quadruplex was clearly evidenced in Tris/KCl buffer. Single-stranded or stem-loop structure was proposed for the Tris buffer medium. An intermediate situation was probable in Tris/NaCl buffer, where intramolecular hairpins might form interstrand quadruplexes. The T_m values of the human telomeric sequence obtained in Tris/KCl or in Tris/NaCl buffers were respectively of 51 or 38 °C indicating also clearly that the structures of DNA were different in these two experimental conditions.

We tested the reactivity of the Mn-TMPyP/$KHSO_5$ nuclease onto the human telomeric sequence under the three conditions (Tris/KCl, Tris/NaCl or Tris alone).

Cleavage of the Human Telomeric Sequence by Mn-TMPyP/$KHSO_5$ Depends on the Secondary Structures. Mn-TMPyp interacted with the human telomeric sequence as shown by the increase of the melting temperature measured in Tris/KCl or in Tris/NaCl buffers. Under the conditions used for the cleavage assays (see below) the Mn-TMPyP induced an increase of 6−7 °C of the T_m in both salted buffers.

The oxidative reactivity of the manganese porphyrin toward the human telomeric sequence was assayed with the telomeric target at 1 μM concentration in the presence of 1 μM of Mn-TMPyP (one molecule of porphyrin for one telomeric sequence) in Tris/KCl, Tris/NaCl, and in Tris buffer. Initiation of the reaction was achieved by addition of $KHSO_5$ (final concentration 100 μM). The reaction time was 1 h (or 5 min) at 0 °C. The resulting products were analyzed by electrophoresis on a 20% denaturing polyacrylamide gel (Figure 4). In the absence of piperidine treatment no significant degradation was observed whatever the conditions (Tris/KCl, Tris/NaCl, and Tris) (Figure 4A, lanes 1−3). Some broad bands and smears were probably due to multiple oxidative lesions partially transformed into definite strand breaks. This phenomenon was observed previously for guanine lesions mediated by Mn-TMPyP derivatives (*36*). These lesions were revealed as discrete cleavage bands by a piperidine treatment (Figure 4A, lanes 4−6). Only these lanes will be detailed since only piperidine treatment revealed the total oxidative reactivity of the oxo-metalloporphyrin. The piperidine cleavage pattern varied depending on the reaction buffer indicating a different interaction between the metalloporphyrin and the DNA target.

When the oxidation reaction was performed in the presence of K^+ ions (Figure 4A, lane 4), the metalloporphyrin was able to mediate oxidative damage at the T_{10}, T_{11}, G_{12}, T_{21}, T_{22}, and G_{24} residues. In this buffer, if the target DNA formed an intramolecular quadruplex, the observed cleavage sites would be in the vinicity of the last tetrad formed by G_{12}, G_{20}, G_{24}, and G_{32} bases (Figure 5A). This suggested that Mn-TMPyP interacted with the intramolecular quadruplex by a one-side external stacking with the G_{12}-G_{20}-G_{24}-G_{32} last tetrad. Both G_7 and G_8 guanines of the double-stranded region were not touched indicating that the interaction of the metalloporphyrin with the telomeric sequence was stronger than with the double-stranded stem and was governed by the affinity of the metalloporphyrin with the G-tetrad plane. The surprising absence of the metalloporphyrin on the other side of the quadruplex, at the G_{14}-G_{18}-G_{26}-G_{30} tetrad, may be tentatively explained by the presence of two lateral loops that impeded the incoming of Mn-TMPyP at that site. This absence of binding on the "top" side of this quadruplex structure was also observed for the nonmetalated porphyrin, H_2-TMPyP. It was found by molecular modeling studies that the external stacking of H_2-TMPyP with the G_{14}-G_{18}-G_{26}-G_{30} tetrad was extremely unfavorable compared to the interaction on the other side (*25*). Since Mn-TMPyP exhibits two axial ligands, it could not be completely stacked with the bottom G-tetrad as was the case for the nonmetalated H_2-TMPyP. The presence of two axial ligands, one oxo- and one-hydroxo ligand, has been evidenced using ^{18}O-labeling experiments in DNA cleavage mediated by Mn-TMPyP/$KHSO_5$ and involving an oxo-hydroxo tautomerism (*32*, *37*). Thus, in Tris/KCl buffer, the interaction of the manganese porphyrin was found to be different from the interaction of H_2-TMPyP (*22*, *25*). The nonmetalated porphyrin was able to oxidize the four Gs of the last tetrad (G_{12}, G_{20}, G_{24}, and G_{32}) due to a perfect external stacking of the porphyrin plane below these four bases whereas the metalated porphyrin could not penetrate deeply inside the structure due to its axial ligands. Mn-TMPyP reacted preferentially onto the G_{12} and G_{24} guanines of this last tetrad. This fact can be related to the lower oxidation potential of these two guanines that are located at the 5′-position of GGG sequences (*38*, *39*). The G_{20} and G_{32} bases correspond to the G at the 3′-position of GGG sequences and were less sensitive to the oxidation mediated by Mn-TMPyP as was also observed under different oxidation conditions described later.

When the oxidation reaction was performed in the presence of Na^+ ions (Figure 4A, lane 5), some lesions were similar to the ones observed in the presence of K^+ ions: T_{10}, T_{11}, G_{12}, and to a lesser extent G_{24}. These lesions could not be related to the interaction of Mn-TMPyP with an intramolecular quadruplex (Figure 5A) because some of the typical cleavage sites found on such structure in Tris/KCl were missing here, namely the T_{21} and T_{22} sites (see Figure 4A, lane 4). Furthermore, it should be noted the presence of new cleavage sites at positions T_{16} and T_{28}. The reactive sites were thus significantly different when the oxo-metalloporphyrin reacted with the human telomeric sequence in the presence of K^+ or Na^+. This difference could be due to the formation of alternative DNA structures such as three- or six-layered hairpin-dimer DNA in Tris/NaCl (Figure 5B). The interaction of the metalloporphyrin with an external G-quartet within these quadruplex structures can be proposed in a way reminiscent to what has been observed in Tris/KCl. Such mode of interaction leads to the oxidation of T_{28} and T_{16} sites together with G_{12}, T_{10}, and T_{11}. The T_{16} and T_{28} residues are probably not involved in lateral loops anymore as in the case of the intramolecular quadruplex structure shown in Figure 5A, but could be located in single-stranded less rigid regions, leading thus to an increased sensitivity toward the oxidation by the oxo-metalloporphyrin. The T_{21} and T_{22} sites could be located on the middle lateral loop of an intramolecular hairpin precluding its accessibility by the metalloporphyrin. The G_{24} could also be close to this lateral loop and thus will not be touched. The G_{18} and the G_{30} guanine residues are oxidizable due to their positions at the 5′ of GGG sequences but are probably not accessible in the middle of the six-layered hairpin-dimer DNA. In the three-layered hairpin-dimer DNA, the G_{30} base was not

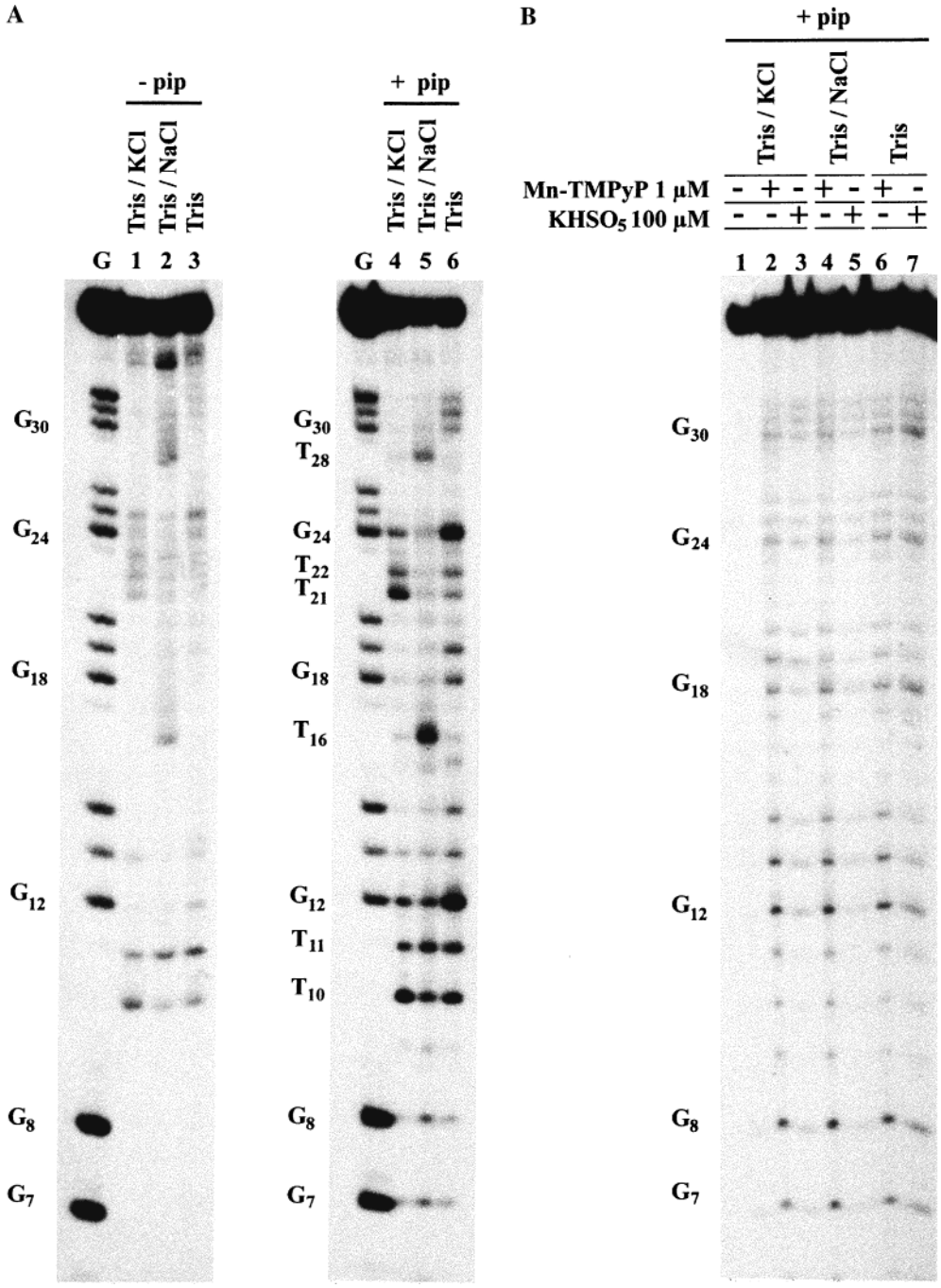

FIGURE 4: (A) PAGE analysis of the oxidative cleavage of the 5′-^{32}P-labeled human telomeric sequence by Mn-TMPyP/$KHSO_5$. Lanes G are the Maxam−Gilbert sequencing reactions. Cleavage reactions were analyzed before (−pip) (lanes 1−3) and after (+pip) (lanes 4−6) piperidine treatment. Oxidation reactions were performed at 0 °C in Tris/KCl (lanes 1 and 4 for 1 h), Tris/NaCl (lanes 2 and 5 for 1 h) or Tris (lanes 3 and 6, for 5 min) buffers. (B) PAGE analysis of the corresponding control experiments of the oxidative cleavage of the 5′-^{32}P-labeled human telomeric sequence by Mn-TMPyP/$KHSO_5$. Controls were done in Tris/KCl (1−3), in Tris/NaCl (lanes 4 and 5) or in Tris (lanes 6 and 7) buffers. All the lanes corresponded to analysis performed after piperidine treatment. Incubation of the labeled DNA alone in Tris/KCl buffer was in lane 1. Control of incubations of DNA with Mn-TMPyP were the lanes 2, 4, and 6. Incubation with KHSO5 were lanes 3, 5, and 7. See Experimental Section for details.

involved in a G-tetrad and this may explain its lack of reactivity. The absence of reactivity of the G_{18} base which might have been associated with the T_{16} lesion (in a way similar to the G_{12} lesion being associated with the T_{10} and T_{11} lesions in the three-layered quadruplex) could not be easily understood. Furthermore, we could observe, as it was the case in the presence of K^+ cations, that the Watson−Crick double-stranded region (G_7 and G_8 guanines) was less cleaved than the quadruplex region, suggesting once again that the metalloporphyrin affinity was higher for the quadruplex section than for the duplex section of the telomeric DNA target studied here. We propose that the human telomeric DNA, in Tris/NaCl buffer, could be a mixture of three- or six-layered hairpin-dimer DNA (Figure 5B). The interaction of the metalloporphyrin with one external G-tetrad within the three-layered hairpin-dimer can lead to the oxidative damage located at T_{16} and T_{28} sites, whereas the interaction of the Mn-TMPyP with one external G-tetrad within the six-layered hairpin-dimer can lead to the oxidative damage located at G_{12}, T_{10}, and T_{11} sites. In the presence of

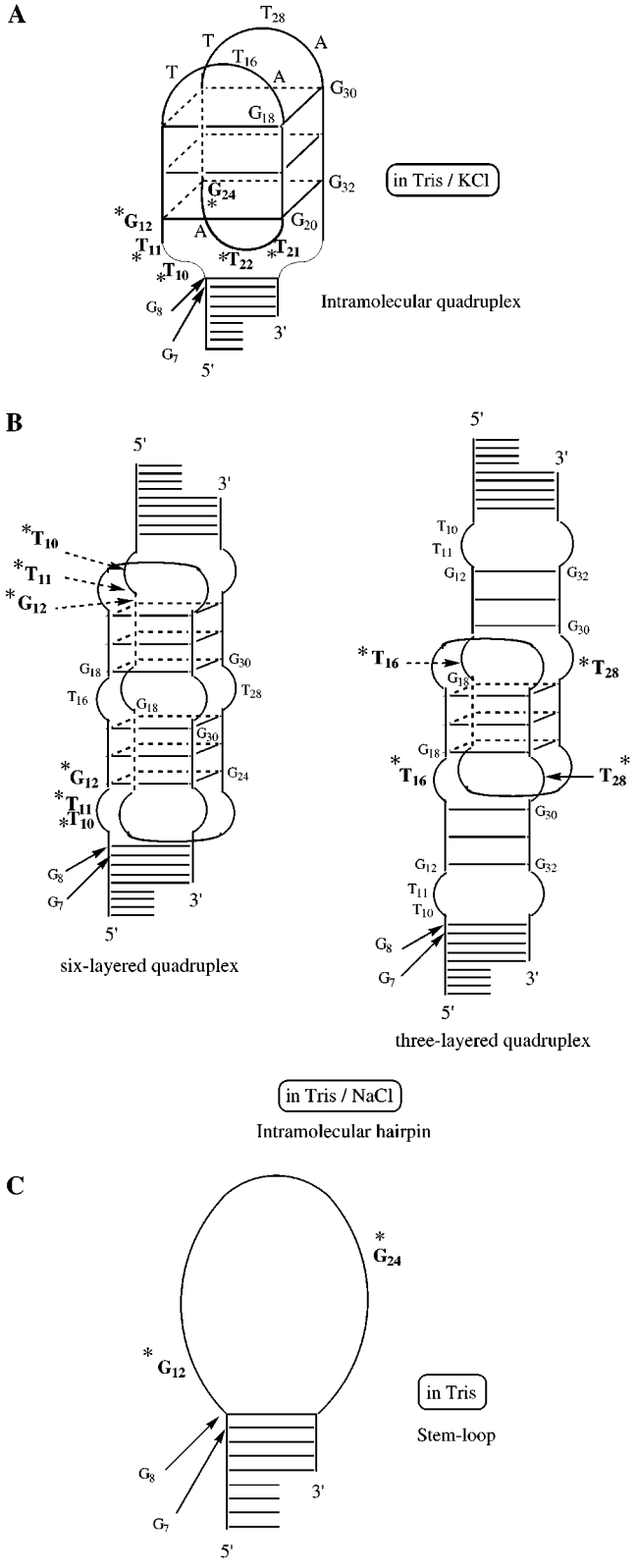

FIGURE 5: Mn-TMPyP/$KHSO_5$ oxidative cleavage sites (indicated by stars) onto hypothetical secondary folding structures of the human telomeric sequence (A) in Tris/KCl buffer, intramolecular quadruplex; (B) in Tris/NaCl buffer, three-or six-layered quadruplexes formed by the association of intramolecular hairpin; and (C) in Tris buffer, simple stem-loop.

Na^+, the interaction of the metalloporphyrin with DNA is probably mainly governed by a strong preference for an external stacking with a bottom G-tetrad of a quadruplex DNA structure.

In the absence of K^+ or Na^+ cations (Figure 4A, lane 6), the cleavage profile was once again completely different, compared to the previous ones (Tris/KCl or Tris/NaCl). The cleavage sites were located at almost all the guanines of the four telomeric repeats. However a higher cleavage intensity was observed on the guanines located at the 5′-position of GGG sequences (see G_{12}, G_{18}, G_{19}, and G_{24}) since these guanines are the more oxidizable ones (*38*, 39). Some thymine residues, T_{10}, T_{11}, T_{21}, and T_{22}, were also oxidized. However, G_{24} and G_{12} were by far the most reactive sites (Figure 5C). The double-stranded region was protected from the oxidation reaction. Under unsalted Tris buffer conditions, the probable absence of secondary structure (stem-loop) made all the guanines of the single-stranded target DNA more accessible to the manganese porphyrin. As a consequence, the oxidation reaction was more efficient since the full length DNA was completely degradated after 1 h of reaction at 0 °C. We thus chosed to present the result of this oxidative cleavage in Figure 4A (lanes 3 and 6) after 5 min of reaction since the target degradation yield was comparable to the two other saline conditions at that time. In Tris/KCl or Tris/NaCl buffers, after only 5 min of reaction, half of the degradation yields were obtained, with the same selectivity (data not shown). This probably reflects a higher freedom of the on/off interactions between the metalloporphyrin and DNA in the case of nonquadruplex structures.

In all cases (Tris/KCl, Tris/NaCl, or Tris), all piperidine cleavage fragments comigrated with Maxam−Gilbert sequencing bands and thus corresponded to fragments bearing a 3′-phosphate terminus. The correspondence of G-bands can be seen in Figure 4A. The correspondence of the T-bands is not shown.

The control experiments are shown in Figure 4B. Only the reaction media after piperidine treatment were loaded on the gel. None of them showed significant cleavage compared to the assays of Figure 4A.

Lesions Observed at the Thymine Level Resulted from an Hydroxylation of the 1′-Carbon of the Deoxyribose Residue. The nature of the DNA oxidation products remained to be elucidated at a molecular level. Only two types of DNA damages were observed, namely at G and T residues. The G alkali-labile lesions strongly suggested that the active manganese-oxo species reacted as a two-electron oxidant of the G-base leading to different G-modified products as was recently reported (*29*, *30*). The T-lesions (T_{10}, T_{11}, T_{21}, and T_{22} in Tris/KCl and T_{10}, T_{11}, T_{16}, and T_{28} in Tris/NaCl) were mostly revealed by the piperidine treatment. However, a few bands at T-residues appeared before the piperidine treatment (Figure 4A, lanes 1−3). An oxidation of the thymine base itself could not be considered because thymine, among the four nucleic bases, has the higher redox potential (*40*, *41*). Thus we hypothesized an oxidation chemistry occurring on the deoxyribose moiety of these thymidine residues. Oxidation of the deoxyriboses of DNA by the Mn-TMPyP/$KHSO_5$ system is well documented (*27*, *28*, *37*, *42*, *43*). High-valent metal-oxo complexes are able to abstract H-atom at different sites of deoxyriboses units, usually at C1′, C4′, or C5′ (*43*−*45*). In fact we found that the major attack site was at C1′ as is described below.

The analysis of the nature of the T-damages in Tris/KCl or Tris/NaCl buffers is shown in Figure 6. The standard oxidation reactions were analyzed after 1 h at 0 °C lanes 1 or 6 for Tris/KCl or Tris/NaCl, respectively. The same media

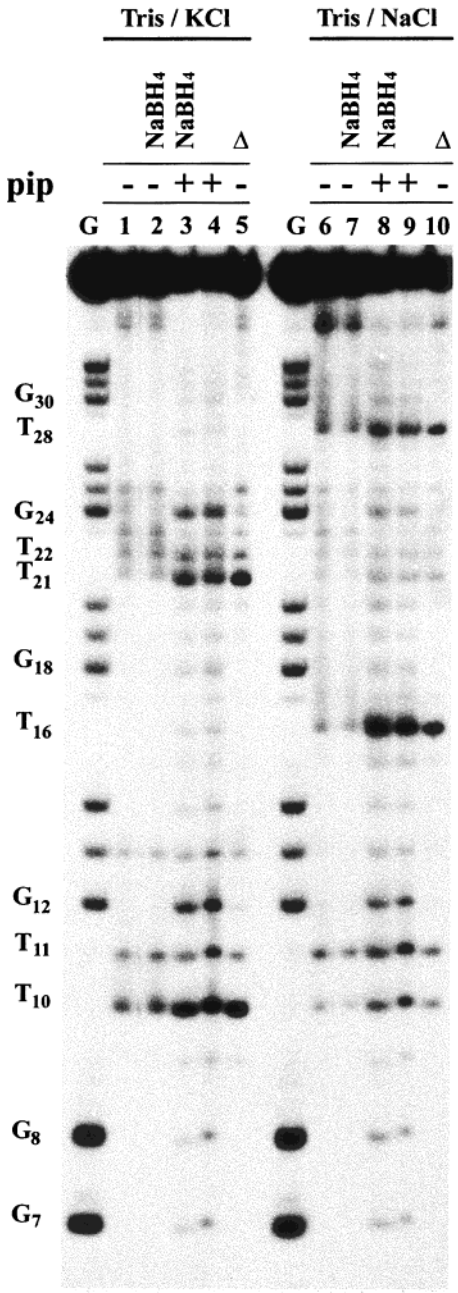

FIGURE 6: PAGE analysis of the oxidation chemistry generating the thymine damages. Lanes G are the Maxam−Gilbert sequencing reactions. Lanes 1 and 4 are classical oxidation reactions performed for 1 h at 0 °C in Tris/KCl buffer respectively before and after a simple piperidine treatment. Lanes 6 and 9 are the same reactions in Tris/NaCl buffer. Lanes 2 and 3 (Tris/KCl) and 7 and 8 (Tris/NaCl) correspond to an oxidation reaction followed by a $NaBH_4$ (0.1 M) reduction before (−pip) and after (+pip) piperidine treatment. Lanes 5 and 10 correspond to a classical oxidation followed by a heating step (30 min at 90 °C) in Tris/KCl and Tris/NaCl, respectively.

were then subjected either to a piperidine treatment, lanes 4 or 9 or to a simple 90 °C heating step, lanes 5 or 10 for Tris/KCl or Tris/NaCl, respectively.

We found that a simple heating step of the cleavage media during 30 min at 90 °C led to the appearance of bands at thymines which were similar in intensity to the ones obtained after piperidine treatment (compare lanes 4 with 5 and lanes 9 with 10, Figure 6). Note that the G lesions did not appear during this simple heating step. This result suggested that the lesions located at the thymidine residues resulted from an oxidation of the 1′-carbon of the deoxyriboses bearing those bases. We previously published that a 90 °C heating step for 30 min at neutral pH resulted in the total release of 5-methylene-2-furanone (5-MF) after two β-eliminations (*27*, *43*) (Scheme 1). In this mechanism, the hydroxylation of the 1′-carbon of the sugar induced the immediate release of the nucleic base and the concomitant formation of a ribonolactone intermediate. The first β-elimination may, at least partially, take place at room temperature (*46*) whereas the second one is heat dependent. We performed an HPLC analysis of the products released during the oxidation of the telomeric DNA. Thymine base was detected before the heating step, and 5-MF was formed during the 90 °C heating step. The products were identified by comparison with authentic standards (*27*, *43*). The main oxidation of the 1′-carbon of the sugars can be explained by the fact that this site is the most oxidizable C−H bond within a sugar moiety.

We must remark that the hydroxylation of the 1′-carbon of deoxyribose units, leading to the ribonolactone intermediate, is not necessarily revealed by piperidine treament (*47*) or thiols treatment (*48*) and was not either completely revealed as direct breaks (*49*). A simple way to evidence this mechanism of sugar oxidation was to perform a 30 min heating step at 90 °C at neutral pH.

Adenine base was also observed on the HPLC chromatogram before the heating step (1 A for 5 T). Since it was not possible to localize these adenine-lesions on the electrophoresis gel, we propose that the metalloporphyrin reacts in the single-stranded sticky end of the telomeric structure which contains one A. The release of adenine base did not increase upon heating. Some exceptions to the oxidation chemistry occurring on the 1′-carbon of deoxyribose were found, the T_{11} site in the case of Tris/KCl buffer (lanes 4 and 5) and T_{10} and T_{11} sites in Tris/NaCl buffer (lanes 9 and 10), whose intensity were not identical upon heating and after piperidine treatment and thus did not involve only a 1′-carbon chemistry. These exceptions to the general 1′-carbon chemistry led us to perform some detection tests to check whether these minor thymidine lesions were due to an oxidation of the 4′- or the 5′-carbon of the sugar.

The direct breaks observed at these sites (lanes 1 and 6, Figure 6), corresponding to 3′-phosphate ending fragments, after 1 h of reaction and without any heating or piperidine treatment could be due to an oxidation of the 5′-carbon (*28*, *43*, *44*). However, a 5′-carbon oxidation cannot account for the total mechanism of oxidative damage at these thymine lesions since the intensity of these lesions increased upon piperidine treatment. Compare the T_{11} band in lanes 1 and 4 of Figure 6 and the T_{10} and T_{11} bands in lanes 6 and 9.

Concerning a contribution of a mechanism involving an oxidation of the 4′-carbon of the sugar (*50*), three different reaction pathways can be observed after abstraction of an H-atom at the 4′-carbon: (i) a trapping of the C-centered radical by dioxygen leading to phosphoglycolate ending fragments of DNA, (ii) a rebound of the metal-hydroxo with the radical to produce a direct hydroxylation and a 4′-hydroxylated abasic site, or (iii) an oxidation of the C-centered radical to a cation which reacts with water and leads to the same 4′-hydroxylated abasic site. We did not obtain any phosphoglycolate-ended fragments which should appear before piperidine treatment but whose migration is known to be different from the one of the 3′-phosphate ending fragments (*43*, *44*, *48*). However, the action of oxo-Mn-

Scheme 1: Mechanism of the Cleavage of DNA by 1′-Carbon Hydroxylation of Deoxyribose by Mn-TMPyP/$KHSO_5$[a]

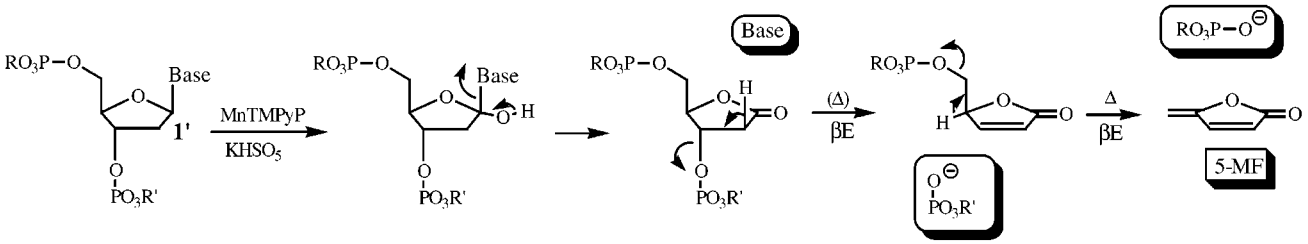

[a] (Δ) Heating step, 90 °C, 30 min at pH 7.5. βE, β-elimination.

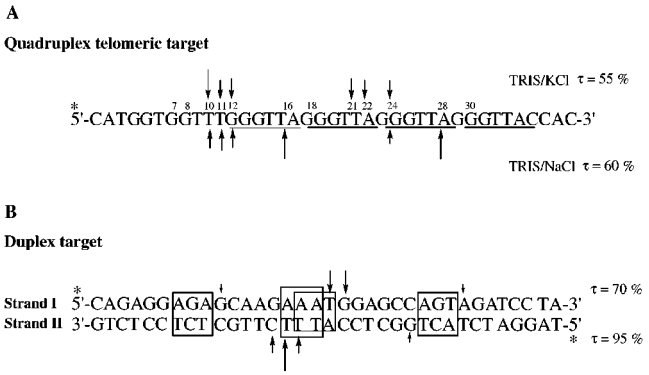

FIGURE 7: Comparison of the Mn-TMPyP/$KHSO_5$ cleavage of (A) quadruplex DNA or (B) duplex DNA. Arrows indicate the sites of selective cleavage, the size of the arrow is proportionnal to the intensity of cleavage. τ indicates the degradation yield of the target determined by the decrease of the intensity of the starting material band after piperidine treatment on electrophoresis gels.

TMPyP could generate product resulting from an hydroxylation at C4′, namely 4′-hydroxylated abasic site (*51*). A $NaBH_4$ treatment is known to prevent the piperidine sensitivity of the 4′-hydroxylated abasic site by reduction of the 1′-aldehyde function. The oxidation reaction medium was treated with $NaBH_4$ and analyzed before and after piperidine treatment. The analysis before piperidine treatment was just a control (Figure 6, lanes 2 and 7, for Tris/KCl and Tris/NaCl, respectively). These lanes were similar to the ones corresponding to standard reaction media without any treatment, lanes 1 and 6 respectively in Figure 6. But the relevant comparison was the analysis of the protecting effect of $NaBH_4$ reduction onto the piperidine induced strand-break of the T-lesions. $NaBH_4$ treatment prior to an alkaline treatment (Figure 6, lane 3 for Tris/KCl and lane 8 for Tris/NaCl) have to be compared with the lanes of simple piperidine treatment (Figure 6, lane 4 for Tris/KCl and lane 9 for Tris/NaCl). The overall similar patterns of lanes 3 and 4 or lanes 8 and 9 in the two different buffers allowed us to confirm that the damages induced by Mn-TMPyP/$KHSO_5$ at the thymine residues did not result from an hydroxylation at the 4′-carbon of the deoxyribose units as major mechanism. However, the T_{11} thymidine damage in Tris/KCl and the T_{10} and T_{11} damages in Tris/NaCl buffer were sensitive to the reducing agent. The piperidine T-bands were less intense after $NaBH_4$ reduction (lanes 3 and 8, Figure 6) compared to the untreated sample band (lanes 4 and 9, Figure 6). Thus a C4′ mechanism occurred at these sites. In summary the exceptions to the C1′ major mechanism of sugar oxidation, at the T_{11} residue in Tris/KCl and the T_{10} and T_{11} residues in Tris/NaCl buffer, were cleaved by C4′- associated to C5′-chemistry. The difference in intensity of piperidine sensitive damage between $NaBH_4$ treated versus untreated lanes indicated the contribution of the minor 4′-oxidation occurring at these sites. The direct breaks observed before any additional treatment can be attributed to oxidation at C5′.

In conclusion, the nature of the oxidative lesions mediated on the human telomeric sequence by Mn-TMPyP/$KHSO_5$ system were not resulting from the same type of oxidation chemistry when located at thymidine or guanosine residues. Oxidation of the base was responsible for guanine lesions while the thymidine lesions were due to an oxidation of the deoxyribose moiety. Hydroxylation of the 1′-carbon of deoxyribose was the major observed mechanism of sugar damage but minor 5′-associated to 4′-carbon oxidation, were found as exceptions (T_{11} in Tris/KCl and T_{10} and T_{11} in Tris/NaCl buffer).

Comparison of the Mn-TMPyP Activity on Duplex DNA and Quadruplex DNA. Mn-TMPyP can specifically interact in the minor groove of double-stranded DNA at discrete sites consisting of three consecutive AT base-pair sequence (*28*). Within this site of high affinity, the oxo-metalloporphyrin is able to oxidize very efficiently the 5′-carbon of the adjacent nucleoside on the 3′-side of the three AT base pairs site thus leading to direct breaks by sugar oxidation (*28*). To compare the Mn-TMPyP/$KHSO_5$ nuclease on quadruplex and duplex DNA (Figure 7), we analyzed the nuclease activity of the manganese porphyrin on a double-stranded DNA model, a 35-mer target. The concentration conditions were the same as those used for the quadruplex oxidation study: the DNA target (1 μM) was incubated with 1 μM of Mn-TMPyP and the reaction was initiated by addition of $KHSO_5$ at a final concentration of 100 μM. The cleavage reaction lasted 1 h at 0 °C. The buffer of the reaction was Tris buffer (50 mM) pH 8, NaCl 100 mM, known to be the most favorable one (*34*). The oxidation reaction induced direct DNA cleavage insensitive to a piperidine treatment. Densitometric analyses showed that the cleavage yield by Mn-TMPyP was 70% on the strand I of the 35-mer target whereas it was 95% on the strand II of the same target (Figure 7). Considering the quadruplex DNA studied above, the cleavage was slightly less efficient. The degradation yield of the human telomeric target was 55 or 60% in the presence of K^+ or Na^+ cations, respectively. Consequently, the oxidative degradation efficiency of Mn-TMPyP/$KHSO_5$ was of the same order toward independent double-stranded or quadruplex DNA structures. These comparative studies of damage mediated by Mn-TMPyP on quadruplex versus duplex structures clearly indicate that metalloporphyrins should be modified in order to improve their targeting toward telomeric quadruplex structures in the search of potent inhibitors of telomerase.

CONCLUSION

Mn-TMPyP/$KHSO_5$ was able to mediate oxidative damage of the human telomeric sequence. The reaction was depend-

ent on the secondary structure formed by the telomeric DNA implying that Mn-TMPyP should be a good probe for the folding topology of quadruplex DNA. A special interaction of the metalloporphyrin with the bottom G-tetrad of a quadruplex DNA has been evidenced. The metalloporphyrin could partially stack on the external side of the last tetrad planar structure provided the single-stranded linker regions were flexible enough to allow the incoming of the metalloporphyrin. Lateral loops seemed to preclude the approach of the metalloporphyrin. Two kinds of oxidative lesions occurred, guanine oxidation within the interacting G-tetrad and mainly 1′-carbon hydroxylation of deoxyriboses carrying thymine bases of the neighboring single-stranded linkers. These results should help to the design of modified metalloporphyrins able to target quadruplex DNA and act as possible telomerase inhibitors.

ACKNOWLEDGMENT

Pr. Jean Bernadou (LCC-CNRS, Toulouse) is acknowledged for fruitful discussions.

SUPPORTING INFORMATION AVAILABLE

Autoradiograms of the gel of DMS footprinting analysis. This material is available free of charge via the Internet at http://pubs.acs.org.

REFERENCES

1. Blackburn, E. H. (1991) *Nature 350*, 569−573.
2. Cech, T. R. (2000) *Angew. Chem., Int. Ed. 39*, 34−43.
3. Moyzis, R. K., Buckingham, J. M., Cram, L. S., Dani, M., Deaven, L. L, Jones, M. D., Meyne, J., Ratliff, R. L., and Wu, J. R. (1988) *Proc. Natl. Acad. Sci. U.S.A. 85*, 6622−6626.
4. Wright, W. E., Tesmer, V. M., Huffman, K. E., Levene, S. D., and Shay, J. W. (1997) *Genes Dev. 11*, 2801−2809.
5. Hardin C. C., Henderson E., Watson T., and Prosser J. K. (1991) *Biochemistry 30*, 4460−4472.
6. Miura, T., and Thomas, G. J., Jr. (1994) *Biochemistry 33*, 7848−7856.
7. Weitzmann, M. N., Woodford, K. J., and Usdin, K. (1996) *J. Biol. Chem. 271*, 20958−20964.
8. Walmsley, J. A., and Burnett, J. F. (1999) *Biochemistry 38*, 14063−14068.
9. Balagurumoorthy, P., and Brahmachari, S. K. (1994) *J. Biol. Chem. 269*, 21858−21869.
10. Williamson, J. R. (1994) *Annu. Rev. Biophys. Biomol. Struct. 23*, 703−730.
11. Lu, M., Guo, Q., and Kallenbach, N. R. (1992) *Biochemistry 31*, 2455−2459.
12. Hud, N. V., Smith, F. W., Anet, F. A. L., and Feigon, J. (1996) *Biochemistry 35*, 15383−15390.
13. Harley, C. B., Futcher, A. B., and Greider, C. W. (1990) *Nature 345*, 458−460.
14. Allsopp, R. C., Vaziri, H., Patterson, C., Goldstein, S., Younglai, E. V., Futcher, A. B., Greider, C. W., and Harley, C. B. (1992) *Proc. Natl. Acad. Sci. U.S.A. 89*, 10114−10118.
15. Counter, C. M., Avilion, A. A., LeFeuvre, C. E., Stewart, N. G., Greider, C. W., Harley, C. B., and Bacchetti, S. (1992) *EMBO J. 11*, 1921−1929.
16. Rhyu, M. S. (1995) *J. Natl. Cancer Inst. 87*, 884−894.
17. Sun, D., Thompson, B., Cathers, B. E., Salazar, M., Kerwin, S. M., Trent, J. O., Jenkins, T. C., Neidle, S., and Hurley, L. H. (1997) *J. Med. Chem. 40*, 2113−2116.
18. Fedoroff, O. Y., Salazar, M., Han, H., Chemeris, V. V, Kerwin, S. M., and Hurley, L. H. (1998) *Biochemistry 37*, 12367−12374.
19. Han, H., Cliff, C. L., and Hurley, L. H. (1999) *Biochemistry 38*, 6981−6986.
20. Guo, Q., Lu, M., Marky, L. A., and Kallenbach, N. R. (1992) *Biochemistry 31*, 2451−2455.
21. Anantha, N. V., Azam, M., and Sheardy, R. D. (1998) *Biochemistry 37*, 2709−2714.
22. Wheelhouse, R. T., Sun, D., Han, H., Han, F. X., and Hurley, L. H. (1998) *J. Am. Chem. Soc. 120*, 3261−3262.
23. Izbicka, E., Wheelhouse, R. T., Raymond, E., Davidson, K. K., Lawrence, R. A., Sun, D., Windle, B. E., Hurley, L. H., and Von Hoff, D. D. (1999) *Cancer Res. 59*, 639−644.
24. Haq, I., Trent, J. O., Chowdhry, B. Z., and Jenkins, T. C. (1999) *J. Am. Chem. Soc. 121*, 1768−1779.
25. Han, F. X., Wheelhouse, R. T., and Hurley, L. H. (1999) *J. Am. Chem. Soc. 121*, 3561−3570.
26. Arthanari, H., Basu, S., Kawano, T. L., and Bolton, P. H. (1998) *Nucleic Acids Res. 26*, 3724−3728.
27. Pratviel, G., Pitié, M., Bernadou, J., and Meunier, B. (1991) *Nucleic Acids Res. 19*, 6283−6288.
28. Pitié, M., Pratviel, G., Bernadou, J., Meunier, B. (1992) *Proc. Natl. Acad. Sci. U.S.A. 89*, 3967−3971.
29. Vialas, C., Pratviel, G., Claparols, C., and Meunier, B. (1998) *J. Am. Chem. Soc. 120*, 11548−11553.
30. Vialas, C., Claparols, C., Pratviel, G., and Meunier, B. (2000) *J. Am. Chem. Soc. 122*, 2157−2167.
31. Bernadou, J., Fabiano, A. S., Robert, A., and Meunier, B. (1994) *J. Am. Chem. Soc. 116*, 9375−9376.
32. Bernadou, J., and Meunier, B. (1998) *Chem. Commun.* 2167−2173.
33. Groves, J. T., Lee, J., and Marla, S. S. (1997) *J. Am. Chem. Soc. 119*, 6269−6273.
34. Bernadou, J., Pratviel, G., Bennis, F., Girardet, M., and Meunier, B. (1989) *Biochemistry 28*, 7268−7275.
35. Wang, Y., and Patel, D. J. (1993) *Structure 1*, 263−282.
36. Mestre, B., Jakobs, A., Pratviel, G., and Meunier, B. (1996) *Biochemistry 35*, 9140−9149.
37. Pitié, M., Bernadou, J., and Meunier, B. (1995) *J. Am. Chem. Soc. 117*, 2935−2936.
38. Sugiyama, H., and Saito, I. (1996) *J. Am. Chem. Soc. 118*, 7063−7068.
39. Saito, I., Nakamura, T., Nakatani, K., Yoshioka, Y., Yamaguchi, K. and Sugiyama, H. (1998) *J. Am. Chem. Soc. 120*, 12686−12687.
40. Jovanovic, S. V., and Simic, M. G. (1986) *J. Phys. Chem. 90*, 974−978.
41. Burrows, C. J., and Muller, J. G. (1998) *Chem. Rev. 98*, 1109−1151.
42. Pratviel, G., Pitié, M., Bernadou, J., and Meunier, B. (1991) *Angew. Chem., Int. Ed. Engl. 30*, 702−704.
43. Pratviel, G., Bernadou, J., and Meunier, B. (1995) *Angew. Chem., Int. Ed. Engl. 34*, 746−769.
44. Pogozelski W. K., and Tullius, T. D. (1998) *Chem. Rev. 98*, 1089−1107.
45. Pratviel, G., Bernadou, J., and Meunier, B. (1998) *Adv. Inorg. Chem. 45*, 251−312.
46. Kappen, L. S., Goldberg, I. H., Wu, S. H., Stubbe, J., Worth, L., Jr., and Kozarich, J. W. (1990) *J. Am. Chem. Soc. 112*, 2797−2798.
47. Chen, T., and Greenberg, M. M. (1998) *J. Am. Chem. Soc. 120*, 3815−3816.
48. Kappen, L. S., and Goldberg, I. H. (1992) *Biochemistry 3*, 9081−9089.
49. Meijler, M. M., Zelenko, O., and Sigman, D. S. (1997) *J. Am. Chem. Soc. 119*, 1135−1136.
50. stubbe, J., and Kozarich, J. W. (1987) *Chem. Rev. 87*, 1107−1136.
51. Aso, M., Kondo, M., Suemune, H., and Hecht S. M. (1999) *J. Am. Chem. Soc. 121*, 9023−9033.

BI000743X